

# Josephson Current through Semiconductor Nanowire with Spin-Orbit Interaction in Magnetic Field

Tomohiro Yokoyama\* and Mikio Eto

Faculty of Science and Technology, Keio University, 3-14-1 Hiyoshi, Kohoku-ku, Yokohama 223-8522, Japan

Yuli V. Nazarov

Kavli Institute of Nanoscience, Delft University of Technology, Lorentzweg 1, 2628 CJ Delft, The Netherlands

(Dated: October 29, 2018)

We theoretically study the DC Josephson effect of a semiconductor nanowire (NW) with strong spin-orbit interaction when a magnetic field is applied parallel to the NW. We adopt a model of single scatterer in a quasi-one-dimensional system for the case of short junctions where the size of normal region is much smaller than the coherent length. In the case of single conduction channel in the model, we obtain analytical expressions for the energy levels of Andreev bound states,  $E_n$ , and supercurrent  $I$ , as a function of phase difference  $\varphi$  between two superconductors. We show the  $0-\pi$  transition by tuning the magnetic field. In the case of more than one conduction channel, we find that  $E_n(-\varphi) \neq E_n(\varphi)$  by the interplay between the spin-orbit interaction and Zeeman effect, which results in finite supercurrent at  $\varphi = 0$  (anomalous Josephson current) and direction-dependent critical current.

PACS numbers:

## I. INTRODUCTION

For spin-based electronics, spintronics, the manipulation of electron spins in semiconductors is an important issue.<sup>1</sup> The strong spin-orbit (SO) interaction in narrow-gap semiconductors, such as InAs and InSb, has attracted a lot of interest in this context.<sup>2</sup> Nanowires (NWs) of such materials have a great potential for the application to the spintronic devices and also to quantum information processing by utilizing the SO interaction.<sup>3-8</sup> Indeed, the electrical manipulation of single electron spins was reported for quantum dots fabricated on the NWs.<sup>6-8</sup> Recently, the proximity effect was intensively examined when NWs are put on superconductors, for the search of Majorana fermions by the combination of SO interaction and magnetic field.<sup>9</sup> The DC Josephson effect was also studied when the NWs are connected to two superconductors (S/NW/S junctions).<sup>10-12</sup> In this paper, we theoretically study the effect of strong SO interaction on the Josephson current through the NWs in a magnetic field, which is closely related to the recent experimental results.<sup>13</sup>

The Josephson current through mesoscopic systems of normal metal or semiconductor has been studied for a long time. At the interfaces between the normal systems and superconductors, the Andreev reflection takes place in which an electron (a hole) is converted to a hole (an electron).<sup>14</sup> As a result, the electron and hole are coherently coupled to each other, forming the Andreev bound states in the normal region around the Fermi level within the superconducting energy gap  $\Delta_0$ . They have discrete energy levels  $E_n$  (Andreev levels).<sup>15,16</sup> In the presence of phase difference  $\varphi$  between the superconductors, the supercurrent  $I(\varphi)$  is carried by the Andreev bound states when the length of the normal region  $L$  is much smaller than the coherent length  $\xi$  (short junction).<sup>16-19</sup>  $\xi = \hbar v_F / (\pi \Delta_0) \equiv \xi_0$  for ballistic systems and  $\xi = (\xi_0 l)^{1/2}$  for diffusive ones, where  $v_F$  is the Fermi velocity and  $l$  is the mean free path. The supercurrent is simply written in terms of the transmission probability  $T_n$  for conduction channel  $n$

( $= 1, 2, \dots, N$ ) in the normal region,

$$I(\varphi) = \frac{e\Delta_0}{2\hbar} \sum_{n=1}^N \frac{T_n \sin \varphi}{[1 - T_n \sin^2(\varphi/2)]^{1/2}}. \quad (1)$$

In Josephson junctions of superconductor / ferromagnet / superconductor (S/F/S), the  $0-\pi$  transition was observed and intensively studied.<sup>20-24</sup> In the  $\pi$ -state, the free energy is minimal at  $\varphi = \pi$ , which stems from the Zeeman splitting by exchange interaction in the ferromagnet. The splitting makes the spin-dependent phase shift for electrons in the propagation through the ferromagnet. Since the Andreev bound states consist of an electron with spin  $\sigma$  and a hole with spin  $-\sigma$ , the Andreev levels are dependent on the spin in the ferromagnet. The  $0-\pi$  transition was observed when its thickness is gradually changed, as a cusp of critical current.<sup>24</sup> A similar transition was recently observed in S/NW/S junctions with fixed length when the Zeeman splitting is tuned by applying a magnetic field parallel to the NW.<sup>13</sup>

The effect of SO interaction is another interesting subject for the DC Josephson effect. It was investigated by a lot of theoretical groups, for normal metal with magnetic impurities,<sup>25</sup> two-dimensional electron gas (2DEG) in semiconductor heterostructures,<sup>26-33</sup> open quantum dots (QDs),<sup>34</sup> QDs with tunnel barriers,<sup>35-40</sup> carbon nanotubes,<sup>41</sup> quantum wires or NWs,<sup>42-44</sup> and others.<sup>45</sup> Even in the absence of magnetic field, the SO interaction splits the spin-degeneracy of the Andreev levels when the phase difference  $\varphi$  is finite.<sup>34,45</sup> In the short junctions, however, the splitting is not observed unless a weak energy-dependence of the scattering by the SO interaction is taken into account.<sup>34,45</sup> In this case, the supercurrent is given by eq. (1), irrespectively of the SO interaction.

The coexistence of the SO interaction and Zeeman effect induces a supercurrent at  $\varphi = 0$ , so-called anomalous Josephson current.<sup>25,27,28,30,37,42</sup> The anomalous current flows in the  $\varphi_0$ -state in which the free energy has a minimum at  $\varphi = \varphi_0$  ( $\neq 0, \pi$ ).<sup>46</sup> The anomalous Josephson current was predicted

when the length of normal region  $L$  is longer than or comparable to the coherent length  $\xi$ . Krive *et al.* derived the anomalous current for long junctions ( $L \gg \xi$ ) with a single conduction channel.<sup>42</sup> Reynoso *et al.* found the anomalous current through a quantum point contact in the 2DEG for  $L \gtrsim \xi$ .<sup>27</sup> They also showed the direction-dependence of critical current when a few conduction channels take part in the transport. In the experiment on the S/NW/S junctions,<sup>13</sup> the direction-dependent supercurrent was observed for samples of  $L \gtrsim \xi$  in a parallel magnetic field, besides the above-mentioned  $0-\pi$  transition. This should be ascribable to the strong SO interaction in the NWs although the anomalous Josephson current was not examined.

In this paper, we study the properties of the supercurrent through NWs with strong SO interaction, focusing on the case of short junctions. We elucidate the anomalous Josephson current and direction-dependent critical current, based on a simple model. In our model, both elastic scatterings by impurities and strong SO interaction in the NWs are represented by a single scatterer in a quasi-one-dimensional system. The number of conduction channels  $N$  is unity or two. The Zeeman effect is taken into account by the spin-dependent phase shift in the propagation through the system.

First, we analyze the model with  $N = 1$ . We calculate the Andreev levels  $E_n$  as a function of  $\varphi$ , which yields the supercurrent  $I(\varphi)$  via eq. (5). We obtain an analytical expression for  $I(\varphi)$  in the absence of SO interaction and clearly show the  $0-\pi$  transition when the magnetic field is tuned. The SO interaction does not change the supercurrent qualitatively in this case. We still find the relation of  $E_n(-\varphi) = E_n(\varphi)$  and that the free energy is minimal at  $\varphi = 0$  or  $\pi$ . We observe no anomalous supercurrent.

Next, we examine the model with  $N = 2$ , in which the inter-channel scattering takes place at the scatterer. The scattering is represented by a random matrix of the orthogonal ensemble in the absence of SO interaction and that of the symplectic ensemble in the strong limit of SO interaction. The ensembles are interpolated for the intermediate strength of SO interaction. We show that the interplay between the SO interaction and magnetic field results in the breaking of  $E_n(-\varphi) = E_n(\varphi)$  for the Andreev levels, in contrast to the case of  $N = 1$ . This leads to the anomalous Josephson current and the direction-dependent current. We believe that our model should be useful to understand the experimental results on S/NW/S Josephson junctions in which a few conduction channels exist in the NWs,<sup>13</sup> as an approach from the limit of short junctions.

The organization of this paper is as follows. In Sec. 2, we explain our model of single scatterer for the S/NW/S Josephson junctions and calculation method of the Andreev levels and supercurrent. Analytical results are given in Sec. 3 for the case of single channel, whereas numerical results are presented in Sec. 4 for the case of two channels. The last section (Sec. 5) is devoted to the conclusions and discussion.

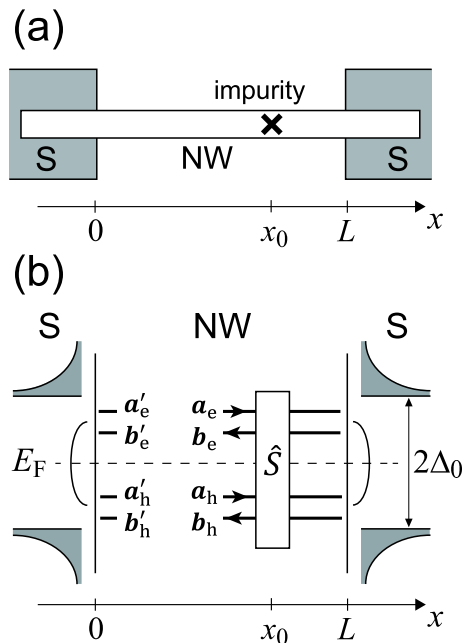


FIG. 1: Our model for a semiconductor nanowire (NW) connected to two superconductors. The NW is represented by a quasi-one-dimensional system along the  $x$  direction, with a single scatterer at  $x = x_0$  to describe the impurity scattering and strong SO interaction. The Zeeman effect is taken into account by the spin-dependent phase shift for a magnetic field applied in the  $x$  direction. (a) Schematic view of the model. The pair potential in the NW is  $\Delta_0 e^{i\varphi_L}$  at  $x < 0$  and  $\Delta_0 e^{i\varphi_R}$  at  $L < x$  by the proximity effect, and 0 at  $0 < x < L$ . (b) The scatterer at  $x = x_0$  is represented by the scattering matrix  $\hat{S}$ .  $a_{e(h)}$  and  $b_{e(h)}$  denote incoming and outgoing electrons (holes) with respect to the scatterer, respectively, whereas  $b'_{e(h)}$  and  $a'_{e(h)}$  are those with respect to the boundary at  $x = 0$  and  $L$ .  $E_F$  is the Fermi energy.

## II. MODEL AND CALCULATION METHOD

In this section, we explain a model of single scatterer in a quasi-one-dimensional system for the NWs. The Bogoliubov-de Gennes (BdG) equation is introduced for the calculation of the Andreev bound states. The formulation of solving the BdG equation is given in terms of the scattering matrix.

### A. Model and BdG equation

Figure 1(a) shows our model in which a NW along the  $x$  direction is connected to two superconductors. At  $x < 0$  and  $L < x$ , the Cooper pairs penetrate into the NW by the proximity effect. They are transported through the normal region of  $0 < x < L$ . The Zeeman effect is taken into account for a parallel magnetic field  $B$  which is so weak as not to break the superconductivity. The Hamiltonian is  $H = H_0 + H_Z$ , with  $H_0 = \mathbf{p}^2/2m + V_{\text{conf}}(y, z) + V_{\text{scatt}}$  and Zeeman effect  $H_Z = g\mu_B \mathbf{B} \cdot \hat{\sigma}/2$ , using effective mass  $m$ ,  $g$ -factor  $g$  ( $< 0$  for InAs and InSb), Bohr magneton  $\mu_B$ , and Pauli matrices  $\hat{\sigma}$ . We take the spin quantization axis along the magnetic field ( $x$

direction).  $V_{\text{conf}}$  describes the confining potential in  $y$  and  $z$  directions. The number of conduction channels is  $N = 1$  or  $2$ .  $V_{\text{scatt}}$  represents both the elastic scattering and SO interaction at a single scatterer at  $x = x_0$ . Its explicit form is given by the scattering matrix in the next subsection. We assume that  $L \ll \xi_0$  and there is no potential barrier at the boundaries between the normal and superconducting regions. Both the Zeeman energy  $E_Z = |g\mu_B B|/2$  and the superconducting energy gap  $\Delta_0$  are much smaller than the Fermi energy  $E_F$ .

To obtain the Andreev bound states, we solve the BdG equation,<sup>47,48</sup>

$$\begin{pmatrix} H - E_F & \hat{\Delta} \\ \hat{\Delta}^\dagger & -(H^* - E_F) \end{pmatrix} \begin{pmatrix} \psi_e \\ \psi_h \end{pmatrix} = E \begin{pmatrix} \psi_e \\ \psi_h \end{pmatrix}, \quad (2)$$

where  $\psi_e = (\psi_{e+}, \psi_{e-})^T$  and  $\psi_h = (\psi_{h+}, \psi_{h-})^T$  are the spinors for electron and hole, respectively. The energy  $E$  is measured from the Fermi level  $E_F$ .  $\hat{\Delta}$  is the pair potential in the spinor space

$$\hat{\Delta} = \Delta(x)\hat{g} = \Delta(x) \begin{pmatrix} & -1 \\ 1 & \end{pmatrix}, \quad (3)$$

where  $\hat{g} = -i\hat{\sigma}_y$ .<sup>48</sup> We assume that  $\Delta(x)$  is  $\Delta_0 e^{i\varphi_L}$  at  $x < 0$ ,  $0$  at  $0 < x < L$ , and  $\Delta_0 e^{i\varphi_R}$  at  $L < x$ . The BdG equation determines the Andreev levels  $E_n$  ( $|E_n| < \Delta_0$ ), as a function of phase difference between the superconductors  $\varphi = \varphi_L - \varphi_R$ .

If the BdG equation has an eigenenergy  $E_n$  with eigenvector  $(\psi_{e,n}, \psi_{h,n})^T$ , it also has the eigenenergy  $-E_n$  with eigenvector  $(\psi_{h,n}^*, \psi_{e,n}^*)^T$ . In short junctions of  $L \ll \xi_0$ , the number of Andreev levels is given by  $4N$ ;  $2N$  positive levels and  $2N$  negative ones when the number of channels is  $N$  ( $2N$  if the spin degrees of freedom is included). The ground state energy is given by

$$E_{\text{gs}}(\varphi) = -\frac{1}{2} \sum_n' E_n(\varphi), \quad (4)$$

where the summation is taken over all the positive Andreev levels,  $E_n(\varphi) > 0$ . The contribution from continuous levels ( $|E| > \Delta_0$ ) is disregarded in eq. (4), which are independent of  $\varphi$  in the short junctions.<sup>16</sup> At zero temperature, the supercurrent is calculated as

$$I(\varphi) = \frac{2e}{\hbar} \frac{dE_{\text{gs}}}{d\varphi} = -\frac{e}{\hbar} \sum_n' \frac{dE_n}{d\varphi}. \quad (5)$$

The current is a periodic function for  $-\pi \leq \varphi < \pi$ . The maximum (absolute value of minimum) of  $I(\varphi)$  yields the critical current  $I_{c,+}$  ( $I_{c,-}$ ) in the positive (negative) direction.

The symmetry of the BdG equation should be noted here. We denote the matrix on the left side of eq. (2) by  $\mathcal{H}(\varphi)$ . In the absence of Zeeman effect,  $\mathcal{T}\mathcal{H}(\varphi)\mathcal{T}^{-1} = \mathcal{H}(-\varphi)$  with the time-reversal operator  $\mathcal{T} = -i\hat{\sigma}_y K$  for spin-1/2 particles. If  $\mathcal{H}(\varphi)$  has an eigenenergy  $E_n$  with eigenvector  $(\psi_{e,n}, \psi_{h,n})^T$ ,  $\mathcal{H}(-\varphi)$  has an eigenenergy  $E_n$  with eigenvector  $\mathcal{T}(\psi_{e,n}, \psi_{h,n})^T$ . Thus the Andreev levels satisfy the relation of  $E_n(\varphi) = E_n(-\varphi)$ . In the absence of SO interaction,  $K\mathcal{H}(\varphi)K^{-1} = \mathcal{H}(-\varphi)$ . Then we derive that  $E_n(\varphi) = E_n(-\varphi)$  in the same way. The relation does not always hold in the presence of both SO interaction and magnetic field.

## B. Formulation using scattering matrix

The BdG equation in eq. (2) is written in terms of the scattering matrix.<sup>16</sup>

First, we represent the effect of  $V_{\text{scatt}}$  by  $\hat{S}_p$  ( $p = e, h$ ): At the scatterer at  $x = x_0$ , an electron is scattered to an electron by  $\hat{S}_e$  and a hole is scattered to a hole by  $\hat{S}_h$ . They connect the amplitudes of incoming particles of  $N$  conduction channels with spin  $\pm$ ,  $(\mathbf{a}_{pL}, \mathbf{a}_{pR})^T$ , and those of outgoing particles,  $(\mathbf{b}_{pL}, \mathbf{b}_{pR})^T$ ,

$$\begin{pmatrix} \mathbf{b}_{pL} \\ \mathbf{b}_{pR} \end{pmatrix} = \hat{S}_p \begin{pmatrix} \mathbf{a}_{pL} \\ \mathbf{a}_{pR} \end{pmatrix}. \quad (6)$$

$\hat{S}_e$  and  $\hat{S}_h$  are  $4N \times 4N$  matrices and related to each other by  $\hat{S}_e(E) = \hat{S}_h^*(-E)$ . On the assumption that they are independent of energy  $E$  for  $|E| < \Delta_0$  and thus  $\hat{S}_e = \hat{S}_h^*$ , we denote  $\hat{S}_e = \hat{S}$  and  $\hat{S}_h = \hat{S}^*$ .  $\hat{S}$  is conventionally written by reflection and transmission matrices:

$$\hat{S} = \begin{pmatrix} \hat{r}_L & \hat{t}_{LR} \\ \hat{r}_{RL} & \hat{t}_R \end{pmatrix}. \quad (7)$$

In addition to the unitarity,  $\hat{S}^\dagger \hat{S} = \hat{1}$ ,  $\hat{S}$  satisfies that  $\hat{r}_L^T = \hat{g}^\dagger \hat{r}_L \hat{g}$ ,  $\hat{r}_R^T = \hat{g}^\dagger \hat{r}_R \hat{g}$ , and  $\hat{t}_{RL}^T = \hat{g}^\dagger \hat{t}_{LR} \hat{g}$  when the time reversal symmetry holds.

Second, we describe the transport of an electron (a hole) in  $0 < x < x_0$  and  $x_0 < x < L$  by scattering matrix  $\hat{\tau}_B$  ( $\hat{\tau}_B^*$ ), considering the Zeeman effect  $H_Z$ . For  $|E| \ll E_F$ , we use a linearized dispersion relation,  $E = +\hbar v_F(k - k_F)$  for  $k > 0$  and  $E = -\hbar v_F(k + k_F)$  for  $k < 0$ , where  $k_F$  is the Fermi wavenumber. For spin  $\sigma = \pm 1$ , the wavefunction is  $\psi_{e,h} \propto e^{ikx}$ , where  $k = k_F + (E \pm E_Z)/(\hbar v_F)$  for  $k > 0$  and  $k = -k_F - (E \pm E_Z)/(\hbar v_F)$  for  $k < 0$ .<sup>49</sup> In the Andreev bound states, a pair of right-going (left-going) electron with spin  $\sigma = \pm 1$  and left-going (right-going) hole with spin  $\sigma = \mp 1$  acquire the phase of  $\pm\theta_{BL}$  with

$$\frac{1}{2}\theta_{BL} = \frac{|g|\mu_B B}{2\hbar v_F} x_0 \quad (8)$$

in the propagation at  $0 < x < x_0$ , and  $\pm\theta_{BR}$  with

$$\frac{1}{2}\theta_{BR} = \frac{|g|\mu_B B}{2\hbar v_F} (L - x_0) \quad (9)$$

in the propagation at  $x_0 < x < L$ . We can safely disregard the phases of  $2Ex_0/(\hbar v_F)$  and  $2E(L - x_0)/(\hbar v_F)$  since  $|E| < \Delta_0$  and  $L \ll \xi_0$ . In the case of two channels ( $N = 2$ ), the Fermi velocity is different for the channels. We neglect the difference because it would not qualitatively change our numerical results in Sec. 4.

The spin-dependent phase shift is represented by the scattering matrix for an electron

$$\begin{pmatrix} \mathbf{b}'_{eL} \\ \mathbf{b}'_{eR} \end{pmatrix} = \hat{\tau}_B \begin{pmatrix} \mathbf{b}_{eL} \\ \mathbf{b}_{eR} \end{pmatrix}, \quad (10)$$

where  $(\mathbf{b}'_{eL}, \mathbf{b}'_{eR})^T$  are amplitudes of outgoing electrons at  $x = 0$  or  $x = L$  [Fig. 1(b)]. It is

$$\hat{\tau}_B = \begin{pmatrix} \hat{1} \otimes \hat{\tau}_{BL} & \\ & \hat{1} \otimes \hat{\tau}_{BR} \end{pmatrix}, \quad (11)$$

where

$$\hat{\tau}_{BL(R)} = \begin{pmatrix} e^{i\theta_{BL(R)}/2} & \\ & e^{-i\theta_{BL(R)}/2} \end{pmatrix} \quad (12)$$

and  $\hat{\Gamma}$  is the  $N \times N$  unit matrix. In our model, the Zeeman effect is characterized by two parameters. One is its strength,

$$\theta_B = \theta_{BL} + \theta_{BR} = \frac{|g|\mu_B B}{\hbar v_F} L = \frac{2E_Z}{E_{Th}}, \quad (13)$$

where  $E_{Th} = \hbar v_F/L$  is the Thouless energy for the ballistic systems. The other is an asymmetry between  $\theta_{BL}$  and  $\theta_{BR}$ ,  $\alpha_B = \theta_{BL}/\theta_{BR} = x_0/(L - x_0)$ . We fix at  $\alpha_B = \sqrt{2}$  for the calculations in this paper.

Third, the Andreev reflection at  $x = 0$  and  $L$  is described by scattering matrix  $\hat{r}_{he}$  for the conversion from electron to hole and  $\hat{r}_{eh}$  for that from hole to electron. When an electron with spin  $\sigma$  is reflected into a hole with  $-\sigma$ , it is written as<sup>16</sup>

$$\begin{pmatrix} \mathbf{a}'_{hL} \\ \mathbf{a}'_{hR} \end{pmatrix} = \hat{r}_{he} \begin{pmatrix} \mathbf{b}'_{eL} \\ \mathbf{b}'_{eR} \end{pmatrix}, \quad (14)$$

where

$$\hat{r}_{he} = e^{-i\alpha} \begin{pmatrix} e^{-i\varphi_L} \hat{\Gamma} \otimes \hat{g} & \\ & e^{-i\varphi_R} \hat{\Gamma} \otimes \hat{g} \end{pmatrix} \quad (15)$$

with  $\alpha = \arccos(E/\Delta_0)$ . When a hole is reflected to an electron, it is

$$\begin{pmatrix} \mathbf{a}'_{eL} \\ \mathbf{a}'_{eR} \end{pmatrix} = \hat{r}_{eh} \begin{pmatrix} \mathbf{b}'_{hL} \\ \mathbf{b}'_{hR} \end{pmatrix} \quad (16)$$

with

$$\hat{r}_{eh} = e^{-i\alpha} \begin{pmatrix} e^{i\varphi_L} \hat{\Gamma} \otimes \hat{g}^\dagger & \\ & e^{i\varphi_R} \hat{\Gamma} \otimes \hat{g}^\dagger \end{pmatrix}. \quad (17)$$

We assume that the channel is conserved at the Andreev reflection in the case of  $N = 2$ . The normal reflection can be neglected in our case without potential barriers at the boundaries of  $x = 0$  and  $L$ .<sup>14</sup>

The total scattering matrix is obtained by the product of  $\hat{S}$ ,  $\hat{\tau}_B$ ,  $\hat{r}_{he}$ , and  $\hat{r}_{eh}$ . The BdG equation yields<sup>16</sup>

$$\det \left( \hat{\Gamma} - \hat{\tau}_B \hat{r}_{eh} \hat{\tau}_B^* \hat{S}^* \hat{\tau}_B \hat{r}_{he} \hat{\tau}_B \hat{S} \right) = 0, \quad (18)$$

which determines the Andreev levels  $E_n(\varphi)$ . In the absence of magnetic field, eq. (18) is simply reduced to<sup>16</sup>

$$\det \left[ 1 - \left( \frac{E}{\Delta_0} \right)^2 - \hat{t}_{LR}^\dagger \hat{t}_{LR} \sin^2 \left( \frac{\varphi}{2} \right) \right] = 0. \quad (19)$$

In this case, the Andreev levels are represented by the transmission eigenvalues of  $\hat{t}_{LR}^\dagger \hat{t}_{LR}$ . They are two-fold degenerate reflecting the Kramers' degeneracy. Thus the Andreev levels  $E_n(\varphi)$  are not split by finite  $\varphi$  in spite of the broken time reversal symmetry.

### III. CALCULATED RESULTS FOR SINGLE CHANNEL

In this section, we present the analytical results for the case of single channel ( $N = 1$ ). In this case, the reflection matrices in eq. (7) are generally written as  $\hat{r}_L = \sqrt{1-T} e^{i\zeta} \hat{\Gamma}$  and  $\hat{r}_R = -\sqrt{1-T} e^{-i\zeta} \hat{\Gamma}$ , where  $T$  is the transmission probability of the scatterer. The phase factor  $e^{i\zeta}$  is cancelled out in eq. (18). The transmission matrices are

$$\hat{t}_{LR} = \sqrt{T} \hat{U}^\dagger \begin{pmatrix} e^{i\eta_{SO}} & \\ & e^{-i\eta_{SO}} \end{pmatrix} \hat{U} \quad (20)$$

and

$$\hat{t}_{RL} = \hat{g}^\dagger \hat{t}_{LR}^T \hat{g} = \sqrt{T} \hat{U}^\dagger \begin{pmatrix} e^{-i\eta_{SO}} & \\ & e^{i\eta_{SO}} \end{pmatrix} \hat{U}, \quad (21)$$

where

$$\hat{U} = \begin{pmatrix} \cos(\theta/2) & \sin(\theta/2) \\ -\sin(\theta/2) & \cos(\theta/2) \end{pmatrix}. \quad (22)$$

The SO interaction is described by the rotation around an axis (effective magnetic field) tilted from the spin quantization axis ( $x$  direction) by  $\theta$ .  $\eta_{SO}$  characterizes the strength of SO interaction;  $0 \leq \eta_{SO} \leq \pi/2$ . The matrix  $\hat{S}$  belongs to the orthogonal ensemble of random matrix theory for  $\eta_{SO} = 0$  (no SO interaction) and to the symplectic ensemble for  $\eta_{SO} = \pi/2$  (strong limit of SO interaction).

#### A. In absence of SO interaction

We begin with the case without SO interaction ( $\eta_{SO} = 0$ ). The  $0-\pi$  transition is elucidated as a function of magnetic field.

By solving eq. (18), we obtain the analytical expression for the Andreev levels

$$\frac{E_{\uparrow\pm}(\varphi)}{\Delta_0} = \cos \left( \frac{\theta_B}{2} + \arccos \left[ \pm \sqrt{(1 + \delta_B + T \cos \varphi)/2} \right] \right), \quad (23)$$

$$\frac{E_{\downarrow\pm}(\varphi)}{\Delta_0} = \cos \left( \frac{\theta_B}{2} - \arccos \left[ \pm \sqrt{(1 + \delta_B + T \cos \varphi)/2} \right] \right), \quad (24)$$

where  $\delta_B = (1 - T) \cos[\theta_B(\alpha_B - 1)/(\alpha_B + 1)]$ . The subscript  $\uparrow$  ( $\downarrow$ ) indicates the state of electron spin  $\sigma = +1$  ( $\sigma = -1$ ) and hole spin  $\sigma = -1$  ( $\sigma = +1$ ). The sign  $\pm$  in eqs. (23) and (24) corresponds to the positive or negative energy at  $\theta_B = 0$ , i.e.  $E_{\uparrow+}(\varphi) = E_{\downarrow+}(\varphi) = -E_{\uparrow-}(\varphi) = -E_{\downarrow-}(\varphi)$  because of the spin degeneracy in the absence of magnetic field. As mentioned in Sec. 2.1, positive and negative levels appear in pairs;  $E_{\uparrow+}(\varphi) = -E_{\downarrow-}(\varphi)$  and  $E_{\downarrow+}(\varphi) = -E_{\uparrow-}(\varphi)$  even for  $\theta_B \neq 0$ . The Andreev levels are an even function of  $\varphi$ ,  $E_n(-\varphi) = E_n(\varphi)$  for  $n = (\uparrow \pm), (\downarrow \pm)$ .

We plot the Andreev levels in eqs. (23) and (24) as a function of  $\varphi$  in Fig. 2(a). The magnetic field gradually increases from  $\theta_B = 0$  to  $\pi$ . We find three regimes for  $\theta_B$ .

(I) In the regime of  $0 \leq \theta_B < \theta_B^{(1)}$ ,  $E_{\uparrow+}, E_{\downarrow+} > 0$  and  $E_{\uparrow-}, E_{\downarrow-} < 0$ . A weak magnetic field splits the Andreev levels

for spin  $\uparrow$  and  $\downarrow$ . With an increase in  $\theta_B$ , the splitting increases and finally  $E_{\uparrow+} = E_{\downarrow-} = 0$  at  $\varphi = \pm\pi$  when  $\theta_B = \theta_B^{(1)}$ . The ground state energy  $E_{\text{gs}}$  in eq. (4) takes a minimum at  $\varphi = 0$  (0-state) in this regime.

(II) When  $\theta_B^{(1)} < \theta_B < \theta_B^{(2)}$ ,  $E_{\uparrow+}(\varphi)$  and  $E_{\downarrow-}(\varphi)$  intersect at  $\varphi = \pm\varphi_1$  and  $E = 0$ ;  $E_{\uparrow+}(\varphi_1) = E_{\downarrow-}(\varphi_1) = 0$ .  $\varphi_1$  satisfies the condition of

$$T \cos \varphi_1 + \cos \theta_B + \delta_B(\theta_B) = 0. \quad (25)$$

With increasing  $\theta_B$ , the intersections move from  $\pm\pi$  ( $\theta_B = \theta_B^{(1)}$ ) to 0 ( $\theta_B = \theta_B^{(2)}$ ).  $\theta_B^{(1)}$  and  $\theta_B^{(2)}$  are determined from  $\cos \theta_B + \delta_B = T$  and  $\cos \theta_B + \delta_B = -T$ , respectively.

(III) When  $\theta_B^{(2)} < \theta_B < \pi$ ,  $E_{\downarrow+}, E_{\downarrow-} > 0$  and  $E_{\uparrow+}, E_{\uparrow-} < 0$ . In this regime,  $E_{\text{gs}}$  is minimal at  $\varphi = \pi$  ( $\pi$ -state). The  $0$ - $\pi$  transition takes place at a critical value of  $\theta_B$  in regime (II).

The behavior of  $E_n(\varphi)$  from  $\theta_B = \pi$  to  $2\pi$  is similar to that from  $\theta_B = \pi$  to 0 in Fig. 2(a). (They are precisely identical to each other in the case of  $x_0 = L/2$ .)

The supercurrent  $I(\varphi)$  is evaluated using eq. (5). In regime (I), it is given by

$$I(\varphi) = \frac{e\Delta_0}{\hbar} \cos\left(\frac{\theta_B}{2}\right) \frac{T \sin \varphi}{\sqrt{2 + 2(\delta_B + T \cos \varphi)}}. \quad (26)$$

This equation coincides with eq. (1) in the absence of magnetic field ( $\theta_B = 0$ ).  $I(\varphi) \propto \sin \varphi$  for  $T \ll 1$ , which is typical for the 0-state. In regime (II),  $I(\varphi)$  is discontinuous at  $\varphi = \pm\varphi_1$ . It is written as

$$I(\varphi) = \begin{cases} \frac{e\Delta_0}{\hbar} \cos\left(\frac{\theta_B}{2}\right) \frac{T \sin \varphi}{\sqrt{2 + 2(\delta_B + T \cos \varphi)}} & (|\varphi| < \varphi_1) \\ -\frac{e\Delta_0}{\hbar} \sin\left(\frac{\theta_B}{2}\right) \frac{T \sin \varphi}{\sqrt{2 - 2(\delta_B + T \cos \varphi)}} & (|\varphi| > \varphi_1) \end{cases}. \quad (27)$$

In regime (III), the supercurrent is continuous and given by

$$I(\varphi) = -\frac{e\Delta_0}{\hbar} \sin\left(\frac{\theta_B}{2}\right) \frac{T \sin \varphi}{\sqrt{2 - 2(\delta_B + T \cos \varphi)}}. \quad (28)$$

$I(\varphi) \propto -\sin \varphi$  for  $T \ll 1$ , which is a character of the  $\pi$ -state. Figure 2(b) exhibits the supercurrent  $I(\varphi)$  as a function of  $\varphi$ . Note that the supercurrent satisfies  $I(-\varphi) = -I(\varphi)$  because  $E_{\text{gs}}(-\varphi) = E_{\text{gs}}(\varphi)$ .

In Fig. 2(c), we plot the critical current as a function of magnetic field. The critical current  $I_{c,+}$  in the positive direction is identical to  $I_{c,-}$  in the negative direction. With increasing  $\theta_B$ ,  $I_{c,\pm}$  decreases first and turns to increase showing a cusp at the critical point of  $0$ - $\pi$  transition. The critical point is around  $\theta_B \sim \pi/2$ , or  $E_Z \sim E_{\text{Th}}$  from eq. (13).

## B. In presence of SO interaction

In the presence of SO interaction ( $\eta_{\text{SO}} \neq 0$ ), the transmission matrix in eq. (20) is rewritten as

$$\hat{t}_{\text{LR}} = \sqrt{T} \begin{pmatrix} e^{i\phi} \sqrt{1 - \epsilon_{\text{SO}}} & i \sqrt{\epsilon_{\text{SO}}} \\ i \sqrt{\epsilon_{\text{SO}}} & e^{-i\phi} \sqrt{1 - \epsilon_{\text{SO}}} \end{pmatrix}, \quad (29)$$

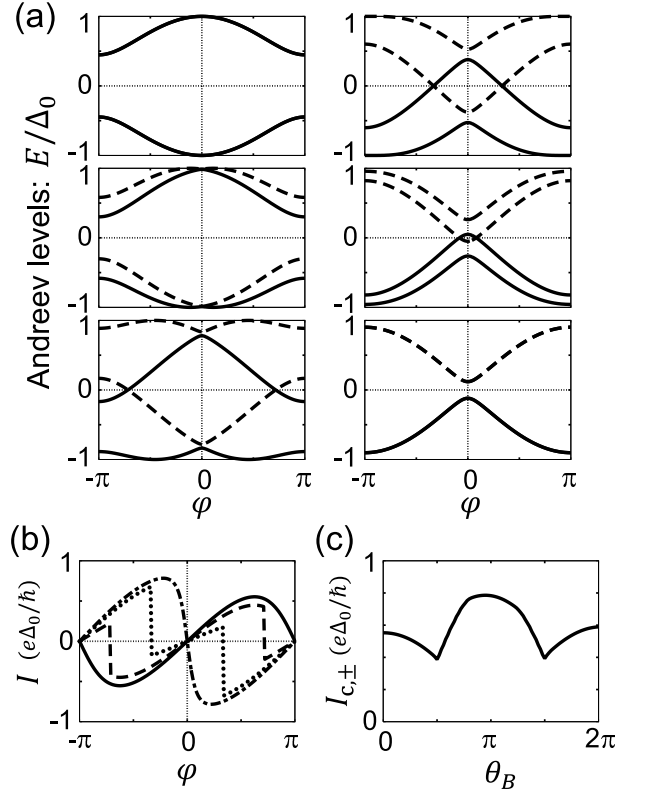


FIG. 2: Calculated result for the model of single conduction channel in the absence of SO interaction ( $N = 1$ ,  $\epsilon_{\text{SO}} = 0$ ). The transmission probability at the scatterer is  $T = 0.8$ . (a) Andreev levels as a function of the phase difference  $\varphi$  between the superconductors,  $E_{\uparrow\pm}$  (solid lines) and  $E_{\downarrow\pm}$  (broken lines). The magnetic field is  $\theta_B = 0$  (left upper),  $0.1\pi$  (left middle),  $0.4\pi$  (left bottom),  $0.7\pi$  (right upper),  $0.9\pi$  (right middle), and  $\pi$  (right bottom). At  $\theta_B = 0$ , solid and broken lines are overlapped to each other;  $E_{\uparrow\pm} = E_{\downarrow\pm}$ . At  $\theta_B = \pi$ ,  $E_{\uparrow+} = E_{\uparrow-}$  and  $E_{\downarrow+} = E_{\downarrow-}$ . (b) Supercurrent  $I(\varphi)$  through the NW. The magnetic field is  $\theta_B = 0$  (solid line),  $0.4\pi$  (broken line),  $0.7\pi$  (dotted line), and  $\pi$  (dash-dot-line). (c) Critical current  $I_{c,\pm}$  as a function of magnetic field,  $\theta_B$ . The current in the positive direction  $I_{c,+}$  is identical to that in the negative direction  $I_{c,-}$ .

where  $\epsilon_{\text{SO}} = \frac{\sin^2(\eta_{\text{SO}}) \sin^2 \theta}{\sqrt{1 - \epsilon_{\text{SO}}}}$  and  $\phi = \arccos[\cos(\eta_{\text{SO}})/\sqrt{1 - \epsilon_{\text{SO}}}]$ . Thus the spin-flip probability is equal to  $\epsilon_{\text{SO}}$ . If the effective magnetic field of SO interaction is parallel to the magnetic field ( $\theta = 0$ ),  $\epsilon_{\text{SO}} = 0$  and no spin flip takes place. Since the phase  $\phi$  is irrelevant to the calculation in eq. (18), the effect of SO interaction is described by single parameter  $\epsilon_{\text{SO}}$ .

We calculate the Andreev levels  $E_n(\varphi)$  by solving eq. (18). Figure 3(a) shows the levels as a function of  $\varphi$  when  $\epsilon_{\text{SO}} = 0.2$ . The magnetic field gradually increases from  $\theta_B = 0$  to  $\pi$ . Since the spin states are mixed by the SO interaction,  $\uparrow$  and  $\downarrow$  are not good quantum numbers. However, the influence of the SO interaction is inconspicuous in the case of single channel.

In the absence of magnetic field ( $\theta_B = 0$ ), all  $E_n(\varphi)$  are identical to those in Fig. 2(a) with  $\epsilon_{\text{SO}} = 0$  because the eigenvalues of  $\hat{t}_{\text{LR}}^\dagger \hat{t}_{\text{LR}}$  are  $T$  in eq. (19), irrespectively of  $\epsilon_{\text{SO}}$ , when

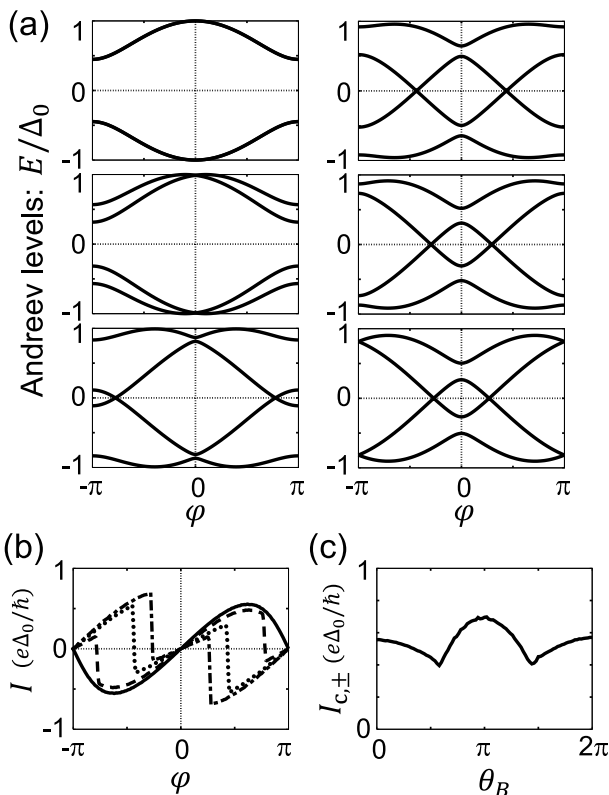


FIG. 3: Calculated result for the model of single conduction channel in the presence of SO interaction ( $N = 1$ ,  $\epsilon_{\text{SO}} = 0.2$ ). The transmission probability at the scatterer is  $T = 0.8$ . (a) Andreev levels  $E_n$  as a function of the phase difference  $\varphi$  between the superconductors. The magnetic field is  $\theta_B = 0$  (left upper),  $0.1\pi$  (left middle),  $0.4\pi$  (left bottom),  $0.7\pi$  (right upper),  $0.9\pi$  (right middle), and  $\pi$  (right bottom). At  $\theta_B = 0$ , two lines are overlapped to each other, reflecting the Kramers' degeneracy. (b) Supercurrent  $I(\varphi)$  through the NW. The magnetic field is  $\theta_B = 0$  (solid line),  $0.4\pi$  (broken line),  $0.7\pi$  (dotted line), and  $\pi$  (dash-dot-line). (c) Critical current  $I_{c,\pm}$  as a function of magnetic field,  $\theta_B$ . The current in the positive direction  $I_{c,+}$  is identical to that in the negative direction  $I_{c,-}$ .

$\hat{t}_{\text{LR}}$  is given by eq. (29). Thus the Andreev levels are not affected by  $\epsilon_{\text{SO}}$ .

The magnetic field splits the Andreev levels. The behavior of the levels with  $\theta_B$  is similar to that in the case of  $\epsilon_{\text{SO}} = 0$ . In regime (I), the splitting is enlarged with an increase in  $\theta_B$ . The 0-state is realized here. In regime (II), the crossing points  $\pm\varphi_1$  of two levels at  $E = 0$  move from  $\pm\pi$  toward 0. The equation for  $\varphi_1$  is modified to

$$T \cos \varphi_1 + \cos \theta_B + \delta_B(\theta_B) = -2T \epsilon_{\text{SO}} \sin\left(\frac{\theta_B}{\alpha_B + 1}\right) \sin\left(\frac{\alpha_B \theta_B}{\alpha_B + 1}\right) \quad (30)$$

by the SO interaction.  $\theta_B^{(1)}$  and  $\theta_B^{(2)}$  satisfy eq. (30) at  $\varphi_1 = \pm\pi$  and  $\varphi_1 = 0$ , respectively. We do not observe regime (III) in Fig. 3(a) since there is no solution for  $\theta_B^{(2)}$  in this case.

The supercurrent is shown in Fig. 3(b) as a function of  $\varphi$ , whereas the critical current is in Fig. 3(c) as a function of  $\theta_B$ . They are qualitatively the same as those in the case of  $\epsilon_{\text{SO}} = 0$ .

In the case of single channel, the relation of  $E_n(-\varphi) = E_n(\varphi)$  holds even in the presence of SO interaction. In consequence the supercurrent satisfies  $I(-\varphi) = -I(\varphi)$  in Fig. 3(b). We do not observe an anomalous Josephson current or direction-dependent critical current:  $I(\varphi = 0) = 0$  and  $I_{c,+} = I_{c,-}$ .

#### IV. CALCULATED RESULTS FOR TWO CHANNELS

In this section, we examine the case of two conduction channels in a NW ( $N = 2$ ) by numerical calculations. We show an anomalous Josephson current and direction-dependent critical current, in contrast to the case of single channel.

For the scattering matrix  $S$  in eq. (7) for a single scatterer at  $x = x_0$ , we prepare random samples following the orthogonal ensemble in the absence of SO interaction and the symplectic ensemble in the strong limit of SO interaction. For the intermediate strength of SO interaction, the ensembles are interpolated with a parameter  $p_{\text{SO}}$  ( $0 \leq p_{\text{SO}} \leq 1$ ), using the method given in Appendix.  $p_{\text{SO}} = 0$  for the orthogonal ensemble and  $p_{\text{SO}} = 1$  for the symplectic ensemble.

First, we present the calculated results for a sample in the absence of SO interaction ( $p_{\text{SO}} = 0$ ) and that in its presence ( $p_{\text{SO}} \neq 0$ ). Then the random average is taken for the latter case.

##### A. In absence of SO interaction

Figure 4(a) shows the Andreev levels as a function of  $\varphi$ , for a sample in the absence of SO interaction ( $p_{\text{SO}} = 0$ ). The magnetic field gradually increases from  $\theta_B = 0$  to  $\pi$ . The levels are labelled as  $E_{\uparrow\pm i}$  (solid line) or  $E_{\downarrow\pm i}$  (broken line) with  $i = 1, 2$  in the same manner as in Sec. 3.1. They appear in pairs,  $E_{\uparrow+i}(\varphi) = -E_{\downarrow-i}(\varphi)$  and  $E_{\downarrow+i}(\varphi) = -E_{\uparrow-i}(\varphi)$ .

When  $\theta_B = 0$ , the Andreev levels are spin-degenerate,  $E_{\uparrow\pm i}(\varphi) = E_{\downarrow\pm i}(\varphi)$ . When  $\theta_B \neq 0$ , we find three regimes for  $\theta_B$  just as before. In regime (I),  $E_{\uparrow+i}, E_{\downarrow+i} > 0$  and  $E_{\uparrow-i}, E_{\downarrow-i} < 0$  although the levels are split by the Zeeman effect. The ground state energy has a minimum at  $\varphi = 0$  (0-state). In regime (II), intersections between  $E_{\uparrow+i}(\varphi)$  and  $E_{\downarrow-i}(\varphi)$  appear at  $E = 0$  for  $i = 1$  only, or both of  $i = 1, 2$ . In regime (III),  $E_{\downarrow\pm i}(\varphi) > 0$  and  $E_{\uparrow\pm i}(\varphi) < 0$ . The  $\pi$ -state is realized in this regime.

In Fig. 4(b), the supercurrent  $I(\varphi)$  behaves almost in the same way as in Fig. 2(b) though  $I(\varphi)$  shows four discontinuities in the case of four intersections in regime (II). Figure 4(c) shows the critical current  $I_{c,\pm}$ , which displays cusps corresponding to the 0- $\pi$  transition at a critical values of  $\theta_B$ . The relation of  $E_n(\varphi) = E_n(-\varphi)$  holds, which yields  $I(\varphi) = -I(-\varphi)$ . Thus we do not observe the anomalous Josephson current or direction-dependence of  $I_{c,\pm}$ .

##### B. In presence of SO interaction

In Fig. 5(a), we present the Andreev levels for a sample in the presence of SO interaction ( $p_{\text{SO}} = 0.3$ ). The interplay

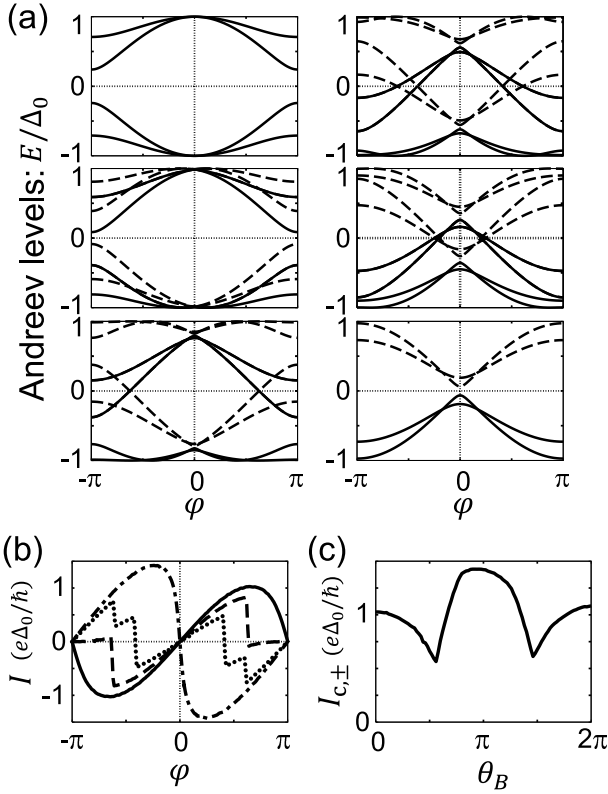


FIG. 4: Calculated result for the model of two conduction channels in the absence of SO interaction ( $N = 2$ ,  $p_{\text{SO}} = 0$ ). A sample is examined for the scattering matrix  $\hat{S}$  at the scatterer. (a) Andreev levels as a function of the phase difference  $\varphi$  between the superconductors,  $E_{\uparrow\pm i}$  (solid lines) and  $E_{\downarrow\pm i}$  (broken lines) with  $i = 1, 2$ . The magnetic field is  $\theta_B = 0$  (left upper),  $0.1\pi$  (left middle),  $0.4\pi$  (left bottom),  $0.6\pi$  (right upper),  $0.8\pi$  (right middle), and  $\pi$  (right bottom). At  $\theta_B = 0$ , solid and broken lines are overlapped to each other;  $E_{\uparrow\pm i} = E_{\downarrow\pm i}$ . At  $\theta_B = \pi$ ,  $E_{\uparrow+i} = E_{\uparrow-i}$  and  $E_{\downarrow+i} = E_{\downarrow-i}$ . (b) Supercurrent  $I(\varphi)$  through the NW. The magnetic field is  $\theta_B = 0$  (solid line),  $0.4\pi$  (broken line),  $0.8\pi$  (dotted line), and  $\pi$  (dash-dot-line). (c) Critical current  $I_{c,\pm}$  as a function of magnetic field,  $\theta_B$ . The current in the positive direction  $I_{c,+}$  is identical to that in the negative direction  $I_{c,-}$ .

between the SO interaction and Zeeman effect leads to a qualitatively new situation.

In the absence of magnetic field ( $\theta_B = 0$ ), the Andreev levels  $E_n(\varphi)$  are two-fold degenerate. The Kramers' degeneracy is not removed by finite  $\varphi$ , as discussed at the end of Sec. 2.2. In the presence of magnetic field, they are split and show that  $E_n(\varphi) \neq E_n(-\varphi)$ . The SO interaction mixes different conduction channels in a spin-dependent way to form the Andreev bound states. This breaks the relation of  $E_n(\varphi) = E_n(-\varphi)$  when  $\theta_B \neq 0$ . Roughly speaking, we can identify three regimes for  $0 < \theta_B < \pi$ , as in Fig. 4. The 0-state appears in regime (I) at  $\theta_B \sim 0$ , whereas  $\pi$ -state is realized in regime (III) at  $\theta_B \sim \pi$ . The 0- $\pi$  transition seems to take place in the intermediate regime. However, we do not observe intersections between the Andreev levels at  $E = 0$  in regime (II). This is due to the anti-crossing of the levels by the SO interaction.

In Fig. 5(b), we show the supercurrent  $I(\varphi)$  as a function

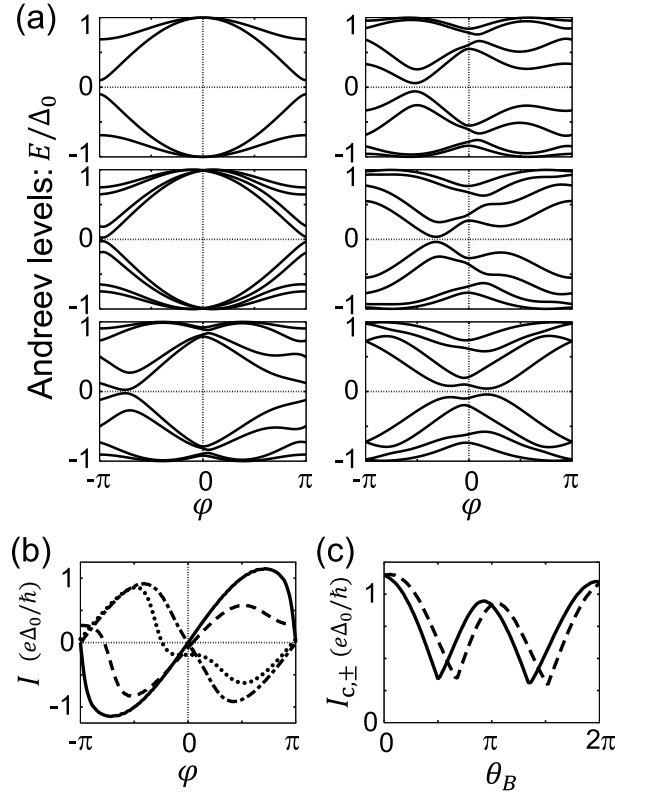


FIG. 5: Calculated result for the model of two conduction channels in the presence of SO interaction ( $N = 2$ ,  $p_{\text{SO}} = 0.3$ ). A sample is examined for the scattering matrix  $\hat{S}$  at the scatterer. (a) Andreev levels  $E_n$  as a function of the phase difference  $\varphi$  between the superconductors. The magnetic field is  $\theta_B = 0$  (left upper),  $0.1\pi$  (left middle),  $0.4\pi$  (left bottom),  $0.6\pi$  (right upper),  $0.8\pi$  (right middle), and  $\pi$  (right bottom). At  $\theta_B = 0$ , two lines are overlapped to each other, reflecting the Kramers' degeneracy. (b) Supercurrent  $I(\varphi)$  through the NW. The magnetic field is  $\theta_B = 0$  (solid line),  $0.4\pi$  (broken line),  $0.8\pi$  (dotted line), and  $\pi$  (dash-dot-line). (c) Critical current as a function of magnetic field  $\theta_B$ ,  $I_{c,+}$  in the positive direction (solid line) and  $I_{c,-}$  in the negative direction (broken line).

of  $\varphi$ .  $I(\varphi) \propto \sin \varphi$  at  $\theta_B = 0$  and  $-\sin \varphi$  at  $\theta_B = \pi$ , which are typical behaviors in the 0-state and  $\pi$ -state, respectively. We do not observe the discontinuity of  $I(\varphi)$  in regime (II), reflecting the absence of intersections of Andreev levels.

It should be stressed that  $I \neq 0$  at  $\varphi = 0$  in Fig. 5(b), indicating the anomalous Josephson current. We plot the anomalous supercurrent  $I(0)$  as a function of  $\theta_B$  in Fig. 6. Since  $E_{\text{gs}}(\varphi) \neq E_{\text{gs}}(-\varphi)$  for the ground state energy,  $I(\varphi) \neq -I(-\varphi)$  for the supercurrent. This results in finite  $I(0)$ . In other words,  $E_{\text{gs}}(\varphi)$  takes a minimum at  $\varphi_0 (\neq 0)$  in regime (I) except  $\theta_B = 0$ . Thus the so-called  $\varphi_0$ -state is realized, where  $I(0) \neq 0$  in eq. (5). Similarly,  $E_{\text{gs}}(\varphi)$  is minimal at  $\varphi_0 (\neq \pi)$  in regime (III). Our numerical result indicates a discontinuous change of  $\varphi_0$  at a value of  $\theta_B$  in regime (II), from  $\varphi_0 \approx 0$  to  $\varphi_0 \approx \pi$ . Therefore, there is a well-defined transition from 0-like-state to  $\pi$ -like-state at the critical value of  $\theta_B$ .

In addition to the anomalous Josephson current, the critical

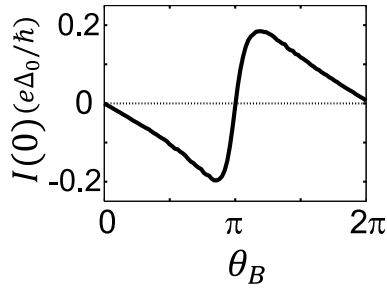


FIG. 6: Supercurrent at  $\varphi = 0$ ,  $I(0)$ , as a function of magnetic field  $\theta_B$ , for the model of two conduction channels in the presence of SO interaction ( $N = 2$ ,  $p_{SO} = 0.3$ ). The sample is the same as that used for Fig. 5.

current depends on its direction. Figure 5(c) shows the current  $I_{c,+}$  in the positive direction (solid line) and  $I_{c,-}$  in the negative direction (broken line), as a function of  $\theta_B$ . Both  $I_{c,+}$  and  $I_{c,-}$  show sharp changes from a decreasing function to an increasing one around  $\theta_B = \pi/2$  and  $3\pi/2$ . The values of  $\theta_B$  at the cusps are different for  $I_{c,+}$  and  $I_{c,-}$ , which are located below and above the critical value of the above-mentioned transition, respectively.

In Figs. 5 and 6, we have presented the results for a sample for the scattering matrix  $\hat{S}$  at the scatterer when  $p_{SO} = 0.3$ . We perform the numerical calculations for 100 samples and take a random average over the samples.

Regarding the anomalous Josephson current,  $I(0)$ , we plot  $\langle I(0) \rangle$  and  $\sqrt{\langle [\Delta I(0)]^2 \rangle}$ , where  $\Delta I(0) = I(0) - \langle I(0) \rangle$ , as a function of  $\theta_B$ , in Fig. 7(a).  $p_{SO} = 0.3$ . The average of anomalous current,  $\langle I(0) \rangle$ , is almost zero since it is positive or negative depending on the samples. Its fluctuation  $\sqrt{\langle [\Delta I(0)]^2 \rangle}$  yields an estimated anomalous current, which is of the order of  $0.1e\Delta_0/\hbar$ . It is zero in the absence of magnetic field ( $\theta_B = 0$ ), increases with  $\theta_B$ , and becomes maximal around  $\theta_B = \pi$ . Then it decreases with  $\theta_B$  until  $\theta_B \approx 2\pi$ .

Figure 7(b) shows  $\sqrt{\langle [\Delta I(0)]^2 \rangle}$  at  $\theta_B = \pi$  (solid line) and  $\theta_B = 0.8\pi$  (broken line), as a function of the strength of SO interaction,  $p_{SO}$ . The anomalous Josephson current increases almost linearly with  $p_{SO}$  for small  $p_{SO}$ . It should be observable when  $p_{SO} \gtrsim 0.05$ .

Next, we examine the direction-dependence of the critical current,  $\delta I_c = I_{c,+} - I_{c,-}$ . Figure 7(c) plots its random average  $\langle \delta I_c \rangle$  and fluctuation  $\sqrt{\langle [\Delta(\delta I_c)]^2 \rangle}$ , where  $\Delta(\delta I_c) = \delta I_c - \langle \delta I_c \rangle$ .  $p_{SO} = 0.3$ . The random average yields  $\langle \delta I_c \rangle \approx 0$ , whereas its fluctuation is of the order of  $0.1e\Delta_0/\hbar$  at  $\pi/2 \lesssim \theta_B \lesssim 3\pi/2$ , where the  $\pi$ -like-state appears.

In Fig. 7(d), we show  $\sqrt{\langle [\Delta(\delta I_c)]^2 \rangle}$  at  $\theta_B = \pi$  (solid line) and  $\theta_B = 0.8\pi$  (broken line), as a function of the strength of SO interaction,  $p_{SO}$ . The direction-dependent supercurrent could be observed when  $p_{SO} \gtrsim 0.05$ .

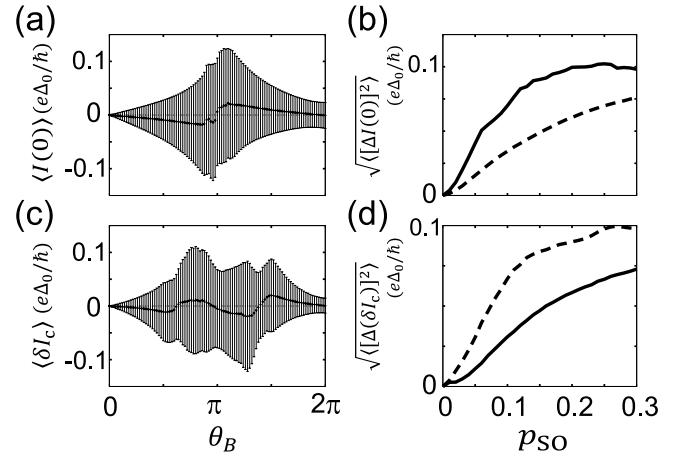


FIG. 7: Calculated result for the model of two conduction channels ( $N = 2$ ). The random average is taken for 100 samples for each strength of SO interaction  $p_{SO}$ . (a) Average of the supercurrent at  $\varphi = 0$ ,  $\langle I(\varphi = 0) \rangle$ , as a function of magnetic field  $\theta_B$ . Error bars represent the average of the fluctuation,  $\sqrt{\langle [\Delta I(0)]^2 \rangle}$ , where  $\Delta I(0) = I(0) - \langle I(0) \rangle$ .  $p_{SO} = 0.3$ . (b)  $\sqrt{\langle [\Delta I(0)]^2 \rangle}$  at  $\theta_B = \pi$  (solid line) and  $\theta_B = 0.8\pi$  (broken line), as a function of the strength of SO interaction,  $p_{SO}$ . (c) Average of the direction-dependence of the critical current,  $\delta I_c = I_{c,+} - I_{c,-}$ , as a function of magnetic field  $\theta_B$ . Error bars represent the average of the fluctuation,  $\sqrt{\langle [\Delta(\delta I_c)]^2 \rangle}$ , where  $\Delta(\delta I_c) = \delta I_c - \langle \delta I_c \rangle$ .  $p_{SO} = 0.3$ . (d)  $\sqrt{\langle [\Delta(\delta I_c)]^2 \rangle}$  at  $\theta_B = \pi$  (solid line) and  $\theta_B = 0.8\pi$  (broken line), as a function of the strength of SO interaction,  $p_{SO}$ .

## V. CONCLUSIONS AND DISCUSSIONS

We have studied the DC Josephson effect in S/NW/S junctions in the presence of strong SO interaction in the NWs and Zeeman effect in a parallel magnetic field. We have examined a simple model of single scatterer in a quasi-one-dimensional system for short junctions where the length of the normal region is much smaller than the coherent length ( $L \ll \xi$ ). For the case of single conduction channel, we have obtained analytical expressions for the Andreev bound states and supercurrent, as a function of phase difference  $\varphi$  between the two superconductors, and derived the  $0-\pi$  transition by tuning the magnetic field. The transition takes place when the Zeeman energy  $E_Z$  is of the order of the Thouless energy  $E_{Th}$  in the ballistic systems. For the case of two conduction channels, we have observed a finite supercurrent at  $\varphi = 0$  (anomalous Josephson current) and direction-dependent critical current due to the interplay between the SO interaction and Zeeman effect. The critical current shows a cusp around the transition between  $0$ - and  $\pi$ -like-states, which is located at different positions for the positive and negative directions, as a function of magnetic field.

Our model indicates the anomalous supercurrent in short junctions with more than one conduction channel, but not with single conduction channel. This is in contrast to the case of long junctions with  $L \gg \xi$ , where the anomalous current is possible even with single channel.<sup>42</sup> However, we cannot ex-



clude that our result is specific to our model where the SO interaction works at a single scatterer.

Recently, the  $0-\pi$  transition and direction-dependent cusps of the critical current were observed in the Josephson junctions of InSb nanowires when a parallel magnetic field is applied.<sup>13</sup> A few conduction channels exist in the NWs, which is similar to the situation of our model, although  $L \gtrsim \xi$  ( $L = 500 \sim 1000$  nm,  $\xi \sim 350$  nm) in the experiment and  $L \ll \xi$  in our model. We are examining an extended model for  $L \gtrsim \xi$  in which the scattering matrices,  $\hat{S}_e$  and  $\hat{S}_h$ , have a weak energy-dependence. Our preliminary result is not qualitatively different from that presented in this paper concerning the case of two channels (anomalous current is possible with single channel in the model for  $L \gtrsim \xi$ ). In the experiment, the spin relaxation length by the SO interaction ( $\xi_{SO} \sim 200$  nm) is comparable to the length of normal region  $L$ . However, it is hard to estimate the parameter  $p_{SO}$  in our model of two conduction channels. We only know that  $p_{SO} = 0$  for  $\xi_{SO}/L \ll 1$  and 1 for  $\xi_{SO}/L \gg 1$ .

#### ACKNOWLEDGMENT

This work was partly supported by a Grant-in-Aid for Scientific Research from the Japan Society for the Promotion of Science. T. Y. is a Research Fellow of the Japan Society for the Promotion of Science. We acknowledge fruitful discussions with Prof. L. P. Kouwenhoven, Dr. S. M. Frolov, Mr. V. Mourik, Mr. K. Zuo in Delft University of Technology, Prof. Y. Nakamura, Prof. S. Tarucha in University of Tokyo, and Dr. K. Ishibashi in RIKEN.

In the case of two channels in the NW, the scattering matrix  $\hat{S}$  in eq. (18) is given randomly to follow the orthogonal ensemble in the absence of SO interaction and the symplectic ensemble in the strong limit of SO interaction. For the intermediate strength of SO interaction, the ensembles are interpolated with a parameter  $p_{SO}$  ( $0 \leq p_{SO} \leq 1$ ), as described below.

For the symplectic ensemble, the scattering matrix is written as a product of a diagonal matrix  $\hat{\Lambda}$  and unitary matrix  $\hat{U}$ ,

$$\hat{S} = \hat{U} \hat{\Lambda} \hat{U}^\dagger. \quad (31)$$

$\hat{\Lambda}$  is given by

$$\hat{\Lambda} = \begin{pmatrix} e^{i\lambda_1} \otimes \hat{1} & & & \\ & \ddots & & \\ & & & e^{i\lambda_{2N}} \otimes \hat{1} \end{pmatrix}, \quad (32)$$

with unit matrix  $\hat{1}$  in the spinor space.  $\lambda_j$  ( $j = 1, 2, \dots, 2N$ ) are given randomly. The unitary matrix  $\hat{U}$  is represented by

$$\hat{U} = (\psi_1, \hat{g}\psi_1^*, \dots, \psi_{2N}, \hat{g}\psi_{2N}^*), \quad (33)$$

where  $2N$  vectors  $\{\psi_j\}$  are complex. They are randomly chosen in such a way that  $\psi_j$  and  $\hat{g}\psi_k^*$  are orthogonal to each other for  $1 \leq j, k \leq 2N$ .

When a matrix in the symplectic ensemble is given, we make a matrix in the orthogonal ensemble as follows. From  $\psi_j$ , a real vector  $\mathbf{x}_j$  is defined as  $\mathbf{x}_j = \text{Re}\psi_j$  for spin component  $\sigma = +1$  and  $\mathbf{x}_j = 0$  for spin component  $\sigma = -1$ . From  $\{\mathbf{x}_j\}$ , an orthonormal set of  $2N$  vectors  $\{\tilde{\mathbf{x}}_j\}$  is created using the Gram-Schmidt orthonormalization. Then we obtain a matrix by eq. (31) with  $\hat{U} = (\tilde{\mathbf{x}}_1, \hat{g}\tilde{\mathbf{x}}_1, \dots, \tilde{\mathbf{x}}_{2N}, \hat{g}\tilde{\mathbf{x}}_{2N})$ , where  $\tilde{\mathbf{x}}_j$  and  $\hat{g}\tilde{\mathbf{x}}_j$  have spin components of  $\sigma = +1$  and  $-1$  only, respectively.

For the intermediate strength of SO interaction, we make

$$\psi'_j = \tilde{\mathbf{x}}_j + p_{SO}(\psi_j - \tilde{\mathbf{x}}_j). \quad (34)$$

We orthonormalize the vectors  $\{\psi'_j, \hat{g}\psi'_j\}$  and construct  $\hat{U}$ . This yields the scattering matrix in eq. (31).

\* E-mail me at: tyokoyam@rk.phys.keio.ac.jp

<sup>1</sup> I. Žutić, J. Fabian, and S. Das Sarma: *Rev. Mod. Phys.* **76**, (2004) 323.

<sup>2</sup> R. Winkler: *Spin-Orbit Coupling Effects in Two-Dimensional Electron and Hole Systems* (Springer, Berlin Heidelberg, 2003).

<sup>3</sup> C. Fasth, A. Fuhrer, L. Samuelson, V. N. Golovach, and D. Loss: *Phys. Rev. Lett.* **98**, (2007) 266801.

<sup>4</sup> A. Pfund, I. Shorubalko, K. Ensslin, and R. Leturcq: *Phys. Rev. B* **79**, (2009) 121306(R).

<sup>5</sup> S. Nadj-Perge, S. M. Frolov, J. W. W. van Tilburg, J. Danon, Yu. V. Nazarov, R. Algra, E. P. A. M. Bakkers, and L. P. Kouwenhoven: *Phys. Rev. B* **81**, (2010) 201305(R).

<sup>6</sup> S. Nadj-Perge, S. M. Frolov, E. P. A. M. Bakkers, and L. P. Kouwenhoven: *Nature* **468**, (2010) 1084.

<sup>7</sup> S. Nadj-Perge, V. S. Pribiag, J. W. G. van den Berg, K. Zuo, S. R. Plissard, E. P. A. M. Bakkers, S. M. Frolov, and L. P. Kouwenhoven: *Phys. Rev. Lett.* **108**, (2012) 166801.

<sup>8</sup> M. D. Schroer, K. D. Petersson, M. Jung, and J. R. Petta: *Phys.*

*Rev. Lett.* **107**, (2011) 176811.

<sup>9</sup> V. Mourik, K. Zuo, S. M. Frolov, S. R. Plissard, E. P. A. M. Bakkers, and L. P. Kouwenhoven: *Science* **336**, (2012) 1003.

<sup>10</sup> Y.-J. Doh, J. A. van Dam, A. L. Roest, E. P. A. M. Bakkers, L. P. Kouwenhoven, and S. De Franceschi: *Science* **309**, (2005) 272.

<sup>11</sup> J. A. van Dam, Yu. V. Nazarov, E. P. A. M. Bakkers, S. De Franceschi, and L. P. Kouwenhoven: *Nature* **442**, (2006) 667.

<sup>12</sup> H. A. Nilsson, P. Samuelsson, P. Caroff, and H. Q. Xu: *Nano Lett.* **12**, (2011) 228.

<sup>13</sup> L. P. Kouwenhoven, S. M. Frolov, V. Mourik, and K. Zuo: private communications.

<sup>14</sup> A. F. Andreev: *Zh. Eksp. Teor. Fiz.* **46**, (1964) 1823; **49**, (1965) 655 [*Sov. Phys. JETP* **19**, (1964) 1228; **22**, (1966) 455].

<sup>15</sup> Y. V. Nazarov and Y. M. Blanter: *Quantum Transport: introduction to nanoscience*, (Cambridge University Press, Cambridge, 2009).

<sup>16</sup> C. W. J. Beenakker: *Phys. Rev. Lett.* **67**, (1991) 3836; *Phys. Rev. Lett.* **68**, (1992) 1442(E).

- <sup>17</sup> J. Bardeen and J. L. Johnson: Phys. Rev. B **5**, (1972) 72.
- <sup>18</sup> A. Furusaki and M. Tsukada: Solid State Commun. **78**, (1991) 299.
- <sup>19</sup> A. Furusaki, H. Takayanagi, and M. Tsukada: Phys. Rev. B **45**, (1992) 10563.
- <sup>20</sup> A. Buzdin: Rev. Mod. Phys. **77**, (2005) 935.
- <sup>21</sup> A. I. Buzdin and M. Y. Kupriyanov: Pis'ma Zh. Eksp. Teor. Fiz. **53**, (1991) 308 [JETP Lett. **53**, (1991) 321].
- <sup>22</sup> T. Kontos, M. Aprili, J. Lesueur, and X. Grison: Phys. Rev. Lett. **86**, (2001) 304.
- <sup>23</sup> V. V. Ryazanov, V. A. Oboznov, A. Yu. Rusanov, A. V. Veretennikov, A. A. Golubov, and J. Aarts: Phys. Rev. Lett. **86**, (2001) 2427.
- <sup>24</sup> V. A. Oboznov, V. V. Bol'ginov, A. K. Feofanov, V. V. Ryazanov, and A. I. Buzdin: Phys. Rev. Lett. **96**, (2006) 197003.
- <sup>25</sup> A. Buzdin: Phys. Rev. Lett. **101**, (2008) 107005.
- <sup>26</sup> E. V. Bezuglyi, A. S. Rozhavsky, I. D. Vagner, and P. Wyder: Phys. Rev. B **66**, (2002) 052508.
- <sup>27</sup> A. A. Reynoso G. Usaj, C. A. Balseiro, D. Feinberg, and M. Avignon: Phys. Rev. Lett. **101**, (2008) 107001.
- <sup>28</sup> J.-F. Liu and K. S. Chan: Phys. Rev. B **82**, (2010) 125305.
- <sup>29</sup> J.-F. Liu, K. S. Chan, and J. Wang: Appl. Phys. Lett. **96**, (2010) 182505.
- <sup>30</sup> J.-F. Liu, K. S. Chan, and J. Wang: J. Phys. Soc. Jpn. **80**, (2011) 124708.
- <sup>31</sup> A. G. Mal'shukov and C. S. Chu: Phys. Rev. B **78**, (2008) 104503.
- <sup>32</sup> A. G. Mal'shukov, S. Sadjina, and A. Brataas: Phys. Rev. B **81**, (2010) 060502(R).
- <sup>33</sup> A. G. Mal'shukov and C. S. Chu: Phys. Rev. B **84**, (2011) 054520.
- <sup>34</sup> B. Béri, J. H. Bardarson, and C. W. J. Beenakker: Phys. Rev. B **77**, (2008) 045311.
- <sup>35</sup> L. Dell'Anna, A. Zazunov, R. Egger, and T. Martin: Phys. Rev. B **75**, (2007) 085305.
- <sup>36</sup> F. Dolcini and L. Dell'Anna: Phys. Rev. B **78**, (2008) 024518.
- <sup>37</sup> A. Zazunov, R. Egger, T. Jonckheere, and T. Martin: Phys. Rev. Lett. **103**, (2009) 147004.
- <sup>38</sup> C. Padurariu and Yu. V. Nazarov: Phys. Rev. B **81**, (2010) 144519.
- <sup>39</sup> C. Karrasch, S. Andergassen, and V. Meden: Phys. Rev. B **84**, (2011) 134512.
- <sup>40</sup> S. Droste, S. Andergassen, and J. Splettstoesser: J. Phys.: Condens. Matter **24**, (2012) 415301.
- <sup>41</sup> J. S. Lim, R. López, and R. Aguado: Phys. Rev. Lett. **107**, (2011) 196801.
- <sup>42</sup> I. V. Krive, L. Y. Gorelik, R. I. Shekhter, and M. Jonson: Low. Temp. Phys. **30**, (2004) 398.
- <sup>43</sup> I. V. Krive, A. M. Kadigrobov, R. I. Shekhter, and M. Jonson: Phys. Rev. B **71**, (2005) 214516.
- <sup>44</sup> M. Cheng and R. M. Lutchyn: Phys. Rev. B **86**, (2012) 134522.
- <sup>45</sup> N. M. Chtchelkatchev and Yu. V. Nazarov: Phys. Rev. Lett. **90**, (2003) 226806.
- <sup>46</sup> H. Sickinger, A. Lipman, M. Weides, R. G. Mints, H. Kohlstedt, D. Koelle, R. Kleiner, and E. Goldobin: Phys. Rev. Lett. **109**, (2012) 107002.
- <sup>47</sup> G. E. Blonder, M. Tinkham, and T. M. Klapwijk: Phys. Rev. B **25**, (1982) 4515.
- <sup>48</sup> The Hamiltonian for the holes would be given by  $-\mathcal{T}H\mathcal{T}^{-1}$ , using the time reversal operator  $\mathcal{T} = -i\hat{\sigma}_y K = \hat{g}K$ , for  $(\phi_{h-}, \phi_{h+})^T$ . In our definition of  $\psi_h$ ,  $\hat{g}$  appears in the off-diagonal part in eq. (2).
- <sup>49</sup> N. M. Chtchelkatchev, W. Belzig, Yu. V. Nazarov, and C. Bruder: JETP Lett. **74**, (2001) 323.